Surface Temperature Measurement from Space: A Case Study in the South Western Cape of South Africa

L.A. Sandham[1] and H.L. Zietsman[2]

1) Department of Geography and Environmental Studies, Potchefstroom University for Christian Higher Education, Private Bag X6001, 2531 Potchefstroom, South Africa

2) Department of Geography and Environmental Studies, University of Stellenbosch, Private Bag X1, 7602 Matieland, South Africa

Submitted for publication: March 1997
Accepted for publication: September 1997
Key words: Surface temperatures, landsat, thematic mapper, South Western Cape, thermal infrared, transformed normalised difference vegetation index

This paper reports on the use of Landsat Thematic Mapper (TM) thermal infrared (TIR) and Transformed Normalised Difference Vegetation Index (TNDVI) data to map summer surface temperature distribution in a portion of the South Western Cape (South Africa). It adopts a ground truth calibration approach, as a possible solution for alleviating the paucity of spatial temperature data. Means and standard deviations of the TIR and transformed NDVI of all pixels within a radius of 120 m around each ground truth point were regressed on spatially collocated surface-observed temperature data. Linear multiple regression analysis showed that mean TIR and standard deviation of TNDVI were effective in accounting for 43% of variation in surface temperature. The regression equation was used to generate a temperature map at a spatial resolution of 30 m, showing good agreement with expected mesoscale spatial temperature patterns in terms of general climatic principles. The temperature map provides a useful tool for depicting and assessing the spatial variation in daily temperatures, providing information currently unavailable to the fruit-producing farmers in the South Western Cape.

Knowledge of land surface temperatures is necessary for a wide range of environmental studies and applications (Kerr, Lanouarde & Imbernon, 1992; Ottlé & Vidal-Madjar, 1992). Applications include climatology and meteorology, soil moisture estimation, forest fire mapping, and investigations into natural vegetation and agriculture (Wan & Dozier, 1989). In agricultural applications, these data are useful *inter alia* in assessing the optimality of production sites and conditions, monitoring the state of the crops and conditions conductive to propagation of pests and diseases, mapping low temperature conditions, and characterising local thermo-topographic conditions in relation to land use (Prata, 1993; Seguin, Courault & Guérif, 1993).

Temperature influences sugar and acid levels in grapes, which in turn influence wine quality (Jackson & Lombard, 1993). Photosynthesis in grapes is 90-100% effective at a temperature range between 18°C and 33°C, and optimal at 25°C-28°C (Van Rensburg, 1992; Jackson & Lombard, 1993). Bergh (1990) showed that the temperature in the 42 days following full bloom has a large influence on size and shape of apples, where weekly increments of fruit growth were proportional to number of weekly hours warmer than 14°C. Bergh (1990) recommends the inclusion of temperature as a variable in predicting harvest size for all apple cultivars. This information could assist in adjusting thinning guidelines as temperatures affect crop levels.

Clearly, knowledge of the spatial and temporal variation of temperatures is particularly important in high-value activities such as viticulture and deciduous fruit production as practised in the South Western Cape, where these agricultural activities are also major employers.

However, due to the high cost of data capture by conventional means (i.e. surface weather stations) and therefore the sparse spatial distribution of weather stations, data on the spatial distribution of temperature are scarce, resulting in poor representation of the spatial temperature field. Advances in satellite remote-sensing techniques offer a fast method of obtaining the spatial distribution of land surface temperatures over large areas, and the availability of high-resolution thermal data from the Landsat Thematic Mapper (TM) allows the investigation of the spatial temperature field at the local scale (Wan & Dozier, 1989).

The utility of satellite data for estimating surface temperatures has been widely investigated for a variety of applications at various scales. Applications at a larger spatial scale include estimation of surface temperatures using NOAA-AVHRR[1] (Kerr *et al.*, 1992; Ottlé & Vidal-Madjar, 1992; Prata, 1993; Seguin *et al.*, 1993). Landsat TM data have been used for application at smaller spatial scales, including: water surface temperature (Lathrop & Lillesand, 1987), analysis of coastal thermal plumes (Gibbons, Wucelic, Leighton & Doyle, 1989), mapping forest fire burns (López García & Caselles, 1991), assessing regional soil moisture conditions (Shih & Jordan, 1993), and investigation of thermal anomalies in active volcanoes (Andres & Rose, 1995).

1 National Oceanic and Atmospheric Administration - Advanced very High Resolution Radiometer

Acknowledgements: Thanks are due to (1) the Institute for Geographical Analysis, Stellenbosch University, for satellite data and processing facilities and (2) the Institute for Soil, Climate and Water (ISCW) of the Agricultural Research Council (ARC).

Satellite data in the thermal infrared range of the electromagnetic spectrum (8-14μm) provide the possibility of deriving temperature data. The basic premise of temperature derivation is Planck's law of black body radiation where emitted thermal radiation is proportional to the temperature of the radiating body. When a sensor measures emitted thermal radiation, the measured values or sensor output (referred to as digital counts - DC) can be converted to temperatures following two main approaches, i.e. (i) ground truth calibration and (ii) internal source calibration.

The ground truth calibration approach requires simultaneous measurement of surface temperatures (ground truth) at several stations concurrent with the satellite overpass. Surface temperature values are correlated to DCs to establish a regression function. This method was used by Lathrop & Lillesand to assess water quality in Lake Michigan (1986) and to map water temperatures (1987), and was also used by López García & Caselles (1991), and Shih & Jordan (1993). Sugita & Brutsaert (1992) used this technique in determining regional fluxes of sensible and latent heat from TM TIR imagery. In this method the atmospheric effects on the remotely sensed thermal IR radiation are inherently taken into account, thus eliminating the need to model or parametrise the complex energy-transfer mechanisms within the surface environment, i.e. soil and canopy, and within the atmosphere (Malaret, Bartolucci, Lozano, Anuta & McGillem, 1985; Bartolucci, Chang, Anuta & Graves, 1988). These mechanisms influence the nature of the radiation reaching the satellite sensor, ultimately determining the degree of accuracy to which the emitted radiation at the surface is sensed at the satellite platform. The major drawback of the ground truth calibration approach is the spatial and temporal limitation of the derived ground truth - DC relationship.

In the internal source calibration approach thermal infrared DCs are converted to temperatures without concurrent ground truth temperature measurements. Satellite on-board calibration values are used to convert DCs to radiance, and atmospheric radiance transmission models such as LOWTRAN and 5S (Moran, Jackson, Slater & Teillet., 1992) are used to account for atmospheric effects on emitted radiation. The corrected radiance values are then converted to surface temperatures by reverse analysis of the Planck equation (Schott & Volchok, 1985; Wukelic, Gibbons, Martucci & Foote, 1989). The atmospheric transfer models in turn require local meteorological data. This approach has been widely investigated and applied (Price, 1983; Schott & Volchok, 1985; Gibbons *et al.,* 1989; Wukelic *et al.,* 1989; Kerr *et al.,* 1992; Moran *et al.,* 1992; Ottlé & Vidal-Madjar, 1992, Prata, 1993; Andres & Rose, 1995).

The advantage of this approach is its independence from concurrent ground truth, and therefore a lesser degree of spatial and temporal limitation and more general utility, but it suffers from the requirement of more complicated routines and the necessity of local radiosonde data for atmospheric correction, as well as the need for accurate values of the emissivity of the surface. Wukelic *et al.* (1989) report large errors where non-local radiosonde data were used. Moreover, information on emissivity of surface features is difficult to determine or not readily available, and small diferences in emissivity of surface features can also cause large errors in estimated surface temperatures (Curran, 1985).

The internal source calibration method is effective, but also expensive and timeconsuming, requiring higher levels of skill, and therefore not always appropriate for robust operational use (Moran *et al.,* 1992).

Since neither surface emissivity values nor local radiosonde data could be obtained, the ground truth calibration approach was regarded as the most suitable method in the exploratory context of this study.

MATERIALS AND METHODS

Study area: The South Western Cape: The South Western Cape region of South Africa is well-known for viticulture and deciduous fruit production, both high-value activities, and therefore very sensitive to any changes in environmental conditions, and thus dependent on the most accurate data available. The area studied in this project comprises the upper Breede River valley, in the general vicinity of the towns of Worcester and Wolseley (Fig. 1). This part of the South Western Cape is characterised by varied topography, with rugged mountains shielding relatively flat, fertile valleys where most of the agricultural activity is located. Spatial and temporal extremes of temperature are characteristic of such areas, with potentially risky consequences for agriculture, emphasising the need for the best available temperature data.

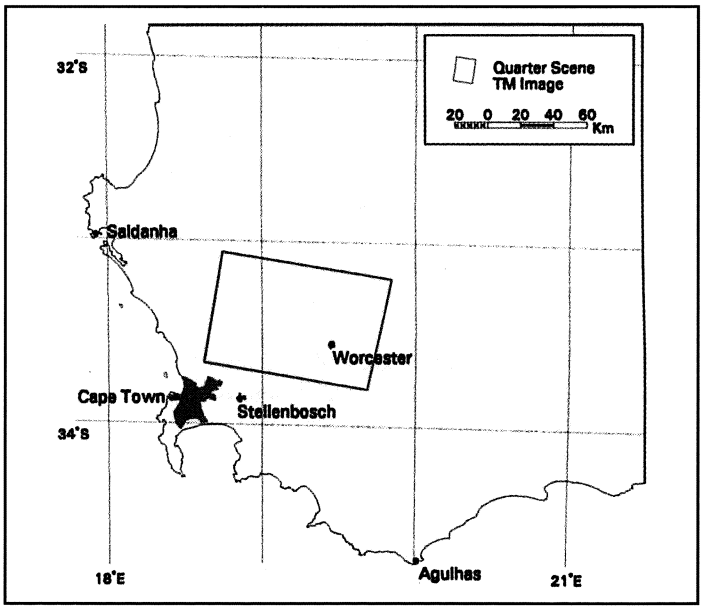

FIGURE 1
Location of study area in the Western Cape.

Ground truth data: These data consisted of hourly temperatures from 12 weather stations within the study area operated by the Institute for Soil, Climate and Water (ISCW) of the Agricultural Research Council (ARC). These are referred to as "surface" temperatures, but are in fact measured in Stevenson screens 1,5 m above the surface.

Satellite data: A Landsat TM quarter (approximately 90 km x 90 km) scanned on 25 Jan 1993 at 09:57 SAST is shown in Fig. 2.

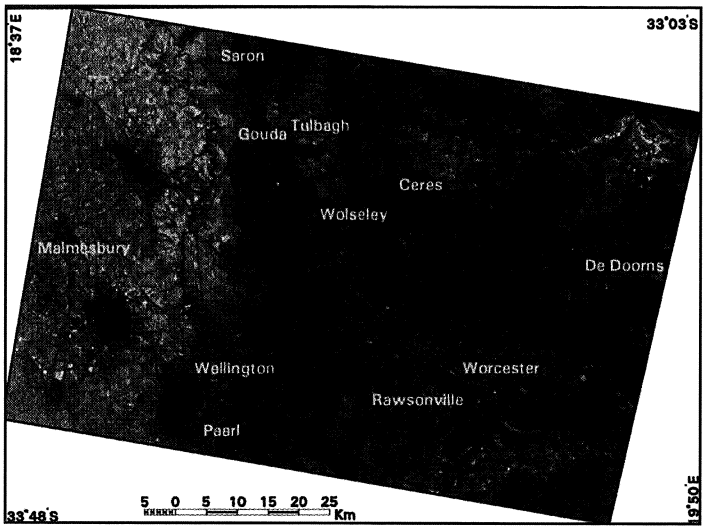

FIGURE 2
LANDSAT TM quarter scene of the study area (25 January 1993).

The Landsat TM scanner provides 30 m spatial resolution in 6 spectral bands, 3 visible and 3 near- to mid-infrared, and 120 m spatial resolution in the thermal infrared band. Spectral band widths appear in Table 1.

TABLE 1

Spectral band widths and colours recorded by the Landsat Thematic Mapper (Curran, 1985).

Band number	Band name	Band width (μm)
1	Blue/green	0,45-0,52
2	Green	0,52-0,60
3	Red	0,63-0,69
4	Near infrared	0,76-0,90
5	Near-middle infrared	1,55-1,75
6	Thermal infrared	10,4-12,5
7	Middle infrared	2,08-2,35

Analysis: Analysis was performed using ERDAS-Imagine and Arc/Info software, resident on two Sunsparc workstations, as well as PC-Statgraphics software. Analysis followed the ground truth calibration approach by which observed surface temperatures were regressed to observed satellite values.

Locations of weather stations were geocoded by longitude and latitude and mapped to a gridded Arc/Info version of the satellite image. Landsat TM scans channel 6 (TIR) in pixels of 120 m, whereas all other channels are scanned in 30 m pixels. For convenience, channel 6 pixels were resampled to 30 m using nearest neighbour resampling in order to preserve original radiance values (DCs). Circular bufers of adjustable radius were then generated around each station to enable extraction of satellite data for corresponding locations. Buffers of different sizes were tested to allow for the influence of possible registration errors as well as environmental effects on measured radiation. To establish the optimal buffer radius, the effects of four different radii were tested, as shown in Table 2.

TABLE 2

Means and standard deviations of TIR for different buffer sizes.

Radius (M)	Pixels in buffer	TIR	TIR
		mean	σ.
30	3,14	111,9	0,479
60	12,00	111,8	1,065
120	50,00	111,6	1,789
240	200,00	111,5	2,818

Satellite TIR values were extracted for each station for each buffer size, and the averages of the means and standard deviations were calculated. From Table 2 it is evident that buffer size exerted minimal influence on the value of the means. This indicated that buffer statistics were not likely to have been distorted by outlier pixel values. As expected, standard deviations increased with radius from 0,479 to 2,818, indicating increasing radiative diversity. It appeared that a radius of 120 m, containing 50 pixels, was optimal, representing a statistically significant sample size, with average standard deviation at 1,79 less than 2% of mean, as well as providing the highest computational efficiency. All further analyses were performed using a buffer radius of 120 m.

Since all of the weather stations did not fall within the area covered by the satellite image, nine stations were used for further analyses. This sample size must be taken into account when interpreting results.

Two types of satellite data were correlated to surface temperatures, i.e. TIR and TNDVI.

1. TIR: As the only form of emitted terrestrial (thermal IR) radiation measured by Landsat, this spectral channel theoretically most closely represents the surface temperature.

2. TNDVI: The transformed normalised difference vegetation index (TNDVI) represents the vegetation biomass and is expressed as the ratio of near-IR reflection (TM channel 4) to red reflection (channel 3), i.e.

$$TNDVI = \sqrt{\frac{(Infrared - Red)}{(Infrared + Red)} + 0,5}$$

i.e. for LandsatTM

$$TNDVI = \sqrt{\frac{(Channel4 - channel3)}{(Channel4 + channel3)}} + 0,5$$

Greenland (1994) expresses TNDVI as *"an integrated function of photosynthesis, leaf area and evapotranspiration"*. The amount of biomass is indirectly and inversely related to surface temperature as a function of a number of interrelated effects, including evapotranspirational cooling, sunlight interception, moisture retention, land cover, the surface energy balance and partial canopy cover (Friedl & Davis, 1994).

Mean and standard deviations of TIR and TNDVI values were calculated for all stations using 120 m buffers. These data were used in linear correlation and regression analysis with surface temperatures. Results are shown in Table 3.

TABLE 3

Correlation matrix of surface hourly temperatures and satellite-derived values.

	TEMPERATURES			TIR		TNDVI	
	10:00	11:00	12:00	mean	σ	mean	σ
TEMP10	1,00	,99	,97	,38	-.09	-,30	-,71
TEMP11		1,00	,99	,44	-,15	-,31	-,72
TEMP12			1,00	,52	-,13	-,36	-,71
TIR Mean				1,00	,34	-,80	-,40
TIR σ					1,00	,36	,14
TNDVI Mean						1,00	,10
TNDVI σ							1,00

Although the Landsat image was scanned at 10:00 SAST, satellite-derived values were correlated to surface temperatures at 10:00, 11:00 and 12:00 to allow for any possible lags between measured temperature and emitted radiation. The rationale here is that surface radiation sensed remotely at 10:00 could be responsible for and therefore most accurately represented by screen temperatures measured at 12:00 (Greenland, 1994).

Satellite values correlated most strongly with 12:00 surface temperatures and on this basis further analysis was performed using 12:00 surface temperatures.

Multiple linear regression was applied using the satellite values as independent variables and 12:00 temperature as the dependent variable. The best multiple regression was obtained for a combination of mean TIR and standard deviation of TNDVI, using R^2 (adjusted for degrees of freedom) as an indicator of the efficacy of regression. The following regression model was obtained:

Temp = 18,3903 - 0,05617 (mean TIR) -47.447 (σTNDVI) with: R = 0,76; R^2 = 0,576; R^2 (adj for d.f.) = 0,435.

When adjusted for degrees of freedom, R^2 = 0,435, i.e. 43% of variation in surface temperature is accounted for by this combination of satellite-derived values. The multiple correlation coefficient is significant at the 90% level.

RESULTS

The derived regression equation was applied to the entire Landsat quarter scene to estimate surface temperature for each pixel. This was an intensive computing process, requiring extraction of a 50 pixel buffer around each pixel (approximately 9 million pixels in the quarter scene) in three different spectral bands, and the calculation of buffer means of TIR and standard deviation of TNDVI (using bands 3 and 4). Only then could the temperature estimation formula be applied to every pixel. Using the FOCALMEANS option in Arc/GRID, this was a simple but time-consuming operation.

The resultant temperature map (Fig. 3) showed a good general agreement with the spatial temperature distribution to be expected and deduced from theoretical principles. Highest temperatures are observed in valleys and lowest temperatures on mountain tops. The temperature map bears a good visual resemblance to both the TIR map (Fig. 4) and the TNDVI map (Fig. 5), even though the TIR values make a relatively small contribution to the temperature in the estimation formula. Perhaps most noticeable is the indication of spatial temperature variation, which cannot be observed on the original false colour image, and would be entirely invisible to the naked eye and on ordinary aerial photography. It would be extremely difficult to monitor these variations by conventional means, and this could only be done at far greater cost than that of satellite imagery. Even with only 40-50% of surface temperature variation explained, this map represents a step forward from interpolating spatial temperature distribution from point values. The value for agriculture is evident.

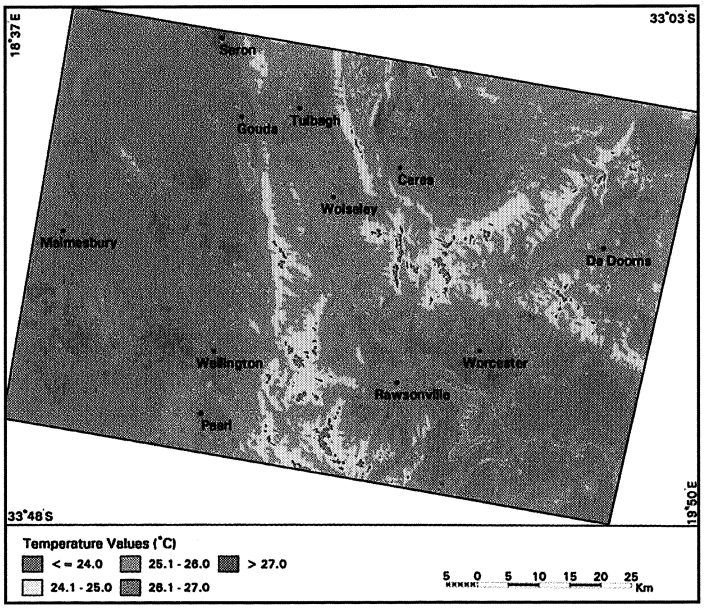

FIGURE 3
Map of estimated surface temperature at 12:00 SAST.

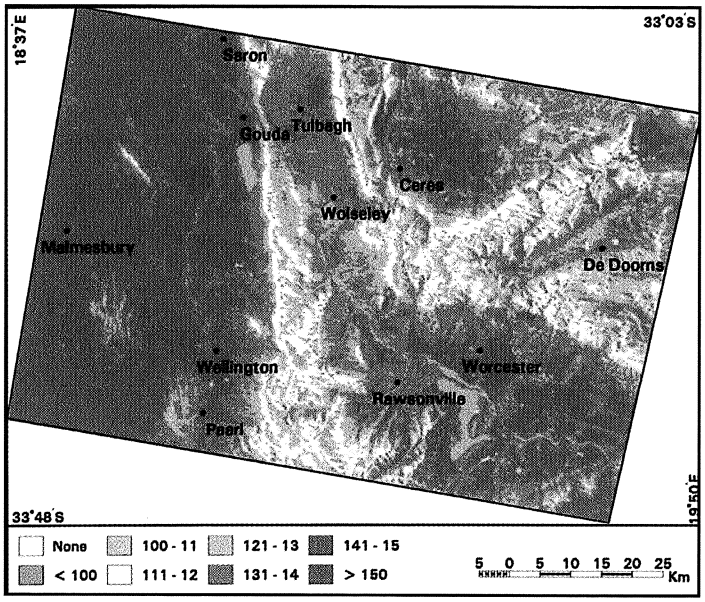

FIGURE 4
Landsat TM Channel 6 thermal infra red image (TIR).

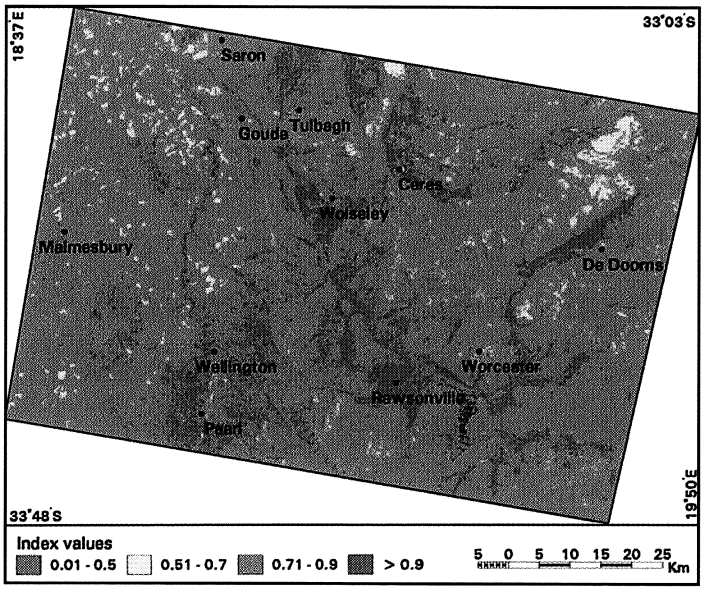

FIGURE 5
Image of Transformed Normalized Difference Vegetation Index (TNDVI).

It must be borne in mind that, although there are differences between absolute and estimated temperatures, the value of TIR is found principally in the interpretation of temperature *patterns* (Curran, 1985), a view supported by Schott and Volchok (1985) *"... TM band 6 data have considerable value in observing the thermal properties of the earth surface but ... caution should be employed where absolute radiance levels are of interest".*

DISCUSSION

With one Landsat in operation, imagery is available every 16 days, although not always cloud-free. Applying a satellite-based temperature estimation model to such imagery in near real-time will enable agriculturists to assess temperature patterns over large areas on a regular basis, and assist in explaining intra-seasonal and spatial anomalies in production rates caused by temperature variations. It also offers useful information for planning the lay-out of new orchards and farms. The advent of increasingly powerful computers and software and the constantly improving access to remotely sensed data place this capability firmly within reach of the agricultural community.

In this study only the summer season was investigated, but more research, including data from the other seasons, and preferably with more widely spread surface temperature data, needs to be undertaken for a better understanding of the TIR - temperature relationship.

LITERATURE CITED

ANDRES, R.J. & ROSE, W.I., 1995. Description of thermal anomalies on two active Guatemalan volcanoes using Landsat Thematic Mapper imagery. *Photogramm Eng. Remote Sens.* **61**(6), 775-782.

BARTOLUCCI, L.A., CHANG, M., ANUTA, P.E. & GRAVES, M.R., 1988. Atmospheric effects on Landsat TM thermal IR data. *IEEE Trans Goesci Remote Sens.* **26**(2), 171-175.

BERGH, O., 1990. Effect of temperature during the first 42 days following full bloom on apple fruit growth and size at harvest. *S. Afr. J. Plant Soil* **7**(1), 11-18.

CURRAN, P.J., 1985. Principles of remote sensing. Longman, Harlow.

FRIEDL, M.A. & DAVIS, F.W., 1994. Sources of variation in radiometric surface temperature over a tallgrass prairie. *Remote Sens. Environ.* **48**, 1-17.

GIBBONS, D.E., WUCELIC, G.E., LEIGHTON, J.P. & DOYLE, M.J., 1989. Application of Landsat Thematic Mapper data for coastal thermal plume analysis at Diablo Canyon. *Photogramm Eng. Remote Sens.* **55**(6), 903-909.

GREENLAND, D., 1994. Use of satellite-based sensing in land surface climatology, *Prog. Physical Geogr.* **18**(1), 1-15.

JACKSON, D.I. & LOMBARD, P.B., 1993. Environmental and management practices affecting grape composition and wine quality - A Review. *Am. J. Enol. Vitic.* **44**(4), 409-430.

KERR, Y.H., LANOUARDE, J.P. & IMBERNON, J., 1992. Accurate land surface temperature retrieval from AVHRR data with use of an improved split window algorithm. *Rem. Sens. Environ.* **41**, 197-209.

LATHROP, R.G. & LILLESAND, T.M., 1986. Use of thematic mapper data to assess water quality in Green Bay and central Lake Michigan. *Photogramm Eng. Remote Sens.* **52**(5), 671-680.

LATHROP, R.G. & LILLESAND, T.M., 1987. Calibration of thematic mapper thermal data for water surface temperature mapping: Case study on the Great Lakes. *Remote Sens. Environ.* **22**, 297-307.

LÓPEZ GARCÍA, M.J. & CASELLES, V., 1991. Mapping burns and reforestation using thematic mapper data. *Geocarto Int.* **1**, 31-37.

MALARET, E., BARTOLUCCI, L.A., LOZANO, D.F., ANUTA, P.E. & McGILLEM, C.D., 1985. Landsat-4 and Landsat-5 Thematic Mapper data quality analysis. *Photogramm Eng. Remote Sens.* **59**(9), 1407-1416.

MORAN, M.S., JACKSON, R.D., SLATER, P.N. & TEILLET, P.M., 1992. Evaluation of simplified procedures for retrieval of land surface reflectance factors from satellite sensor output. *Remote Sens. Environ.* **41**, 169-184.

OTTLÉ, C. & VIDAL-MADJAR, D., 1992. Estimation of land surface temperature with NOAA 9 data, *Remote Sens. Environ.* **40**, 27-41.

PRATA, A.J., 1993. Land surface temperatures derived from the Advanced Very High Resolution Radiometer and the along-track scanning radiometer. 1. Theory. *J. Geophys. Res.* **98**(D9), 16689-16702.

PRICE, J.C., 1983. Estimating surface temperatures from satellite thermal infrared data - a simple formulation for the atmospheric effect. *Remote Sens. Environ.* **13**, 353-361.

SCHOTT, J.R. & VOLCHOK, W.J., 1985. Thematic mapper thermal infrared calibration. *Photogramm Eng. Remote Sens.* **51**(9), 1351-1357.

SEGUIN, B., COURAULT, D. & GUÉRIF, M., 1993. Satellite thermal infrared data applications in agricultural meteorology. *Adv. Space Res.* **13**(5), 207-217.

SHIH, S.F. & JORDAN, J.D., 1993. Use of Landsat Thermal-IR data and GIS in soil moisture assessment. *J. Irrig. Drainage Eng.* **119**(5), 868-879.

SUGITA, M. & BRUTSAERT, W., 1992. Surface temperature derived from mean of pixel radiances without atmospheric correction. *Water Resour. Res.* **28**(6), 1675-1679.

VAN RENSBURG, J., 1992. Invloed van temperatuur op druifsamestelling. *Wynboer Tegnies* **15**, 3.

WAN, Z. & DOZIER, J., 1989. Land-surface temperature measurement from space: Physical principles and inverse modeling, IEEE Trans Geosci *Remote Sens.* **27**(3), 268-277.

WUKELIC, G.E., GIBBONS, D.E., MARTUCCI, L.M. & FOOTE, H.P., 1989. Radiometric calibration of Landsat Thematic Mapper thermal band data. *Remote Sens. Environ.* **28**, 339-347.